Eurographics Symposium on Geometry Processing (2006)
Konrad Polthier, Alla Sheffer (Editors)

On Transfinite Barycentric Coordinates

Alexander Belyaev

Max Planck Institut für Informatik, Saarbrücken, Germany

Abstract

A general construction of transfinite barycentric coordinates is obtained as a simple and natural generalization of Floater's mean value coordinates [Flo03, JSW05b]. The Gordon-Wixom interpolation scheme [GW74] and transfinite counterparts of discrete harmonic and Wachspress-Warren coordinates are studied as particular cases of that general construction. Motivated by finite element/volume applications, we study capabilities of transfinite barycentric interpolation schemes to approximate harmonic and quasi-harmonic functions. Finally we establish and analyze links between transfinite barycentric coordinates and certain inverse problems of differential and convex geometry.

1. Introduction

Design and analysis of transfinite interpolation schemes has been a core research topic in geometric modeling since seminal works of CAGD pioneers [Far02]. More recent interest in transfinite interpolation stems from inventing transfinite versions of classical and modern barycentric coordinates [JSW05b, WSHD06, HF06, SJW06].

The contribution of this paper is threefold. First, we invent a general construction of transfinite barycentric coordinates as a weighted version of transfinite mean value coordinates [Flo03, JSW05b] (Section 2). Next, we analyze relationships between transfinite barycentric interpolation schemes and PDE-based interpolation (Sections 3,4,5). A special attention is paid to approximating harmonic functions (Sections 3,4). In particular, we study and generalize simple and elegant transfinite barycentric coordinates proposed twelve years ago by Gordon and Wixom [GW74] and now almost forgotten (Sections 4,5). Finally, we reveal interesting links between the barycentric interpolation schemes and the famous Christoffel-Minkowski problems studied in differential and convex geometry (Section 6).

After this paper was submitted, we became aware of a recent study [SJW06] where a similar approach to a general construction of 2D transfinite barycentric coordinates was proposed.

While our work is pure theoretical, we believe that the presented results may find applications in computational mechanics and fluid dynamics where numerical methods based on barycentric interpolation schemes gain more and more popularity [AO06, SM06, KFCO06]. Free-form shape deformations constitute another potential area of applications [JSW05b, DM06].

The starting point for our study is a general construction of transfinite barycentric coordinates introduced in [WSHD06]. Given a convex domain Ω, let us consider a smooth function $b(\boldsymbol{x}, \boldsymbol{y})$, $\boldsymbol{x} \in \Omega$ and $\boldsymbol{y} \in \partial\Omega$, satisfying the following three properties

$$\text{Non-negativity} \quad b(\boldsymbol{x}, \boldsymbol{y}) \geq 0, \tag{1}$$

$$\text{Partition of unity} \quad \int_{\partial\Omega} b(\boldsymbol{x}, \boldsymbol{y})\, ds_y = 1, \tag{2}$$

$$\text{Linear precision} \quad \int_{\partial\Omega} \boldsymbol{y}\, b(\boldsymbol{x}, \boldsymbol{y})\, ds_y = \boldsymbol{x}. \tag{3}$$

Now interpolation of function $f(\boldsymbol{y})$ defined on $\partial\Omega$ into Ω is given by

$$f(\boldsymbol{x}) = \int_{\partial\Omega} f(\boldsymbol{y})\, b(\boldsymbol{x}, \boldsymbol{y})\, ds_y. \tag{4}$$

2. Weighted mean value coordinates

The main idea behind the Floater mean value coordinates [Flo03] consists of applying the mean value property for harmonic functions to piecewise linear functions. Consider a convex bounded domain Ω in $\mathbb{R}^n$ and a function $f(\boldsymbol{x})$ harmonic inside Ω

$$\Delta f \equiv \frac{\partial^2 f}{\partial x_1^2} + \ldots + \frac{\partial^2 f}{\partial x_n^2} = 0.$$

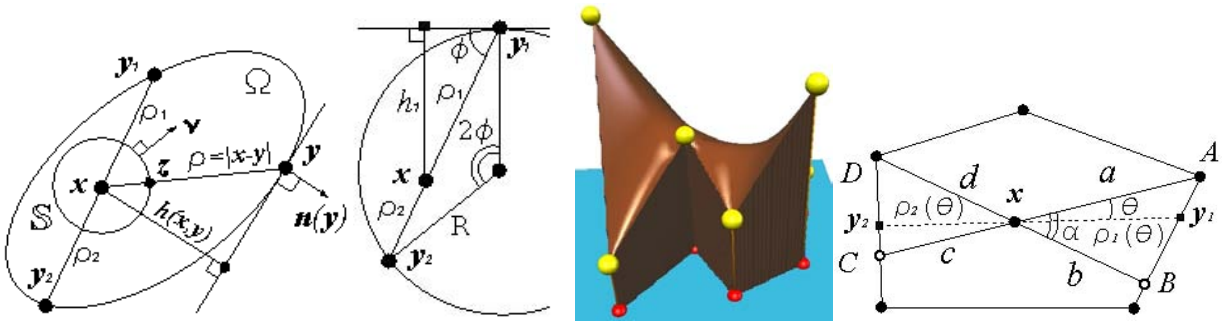

Figure 1: *(a) Main notations employed throughout the paper. (b) Notations used in the proof that certain weighted Gordon-Wixom interpolation schemes are pseudo-harmonic (c) Interpolating inside of a non-convex polygon with the Gordon-Wixom coordinates adapted for non-convex domains. (d) Notations used to derive the Gordon-Wixom coordinates for polygons.*

Let $\boldsymbol{x}$ be a point inside Ω and $S(\boldsymbol{x}, r)$ be the sphere of radius r centered at $\boldsymbol{x}$ and contained inside Ω. Then according to the mean value theorem for harmonic functions

$$f(\boldsymbol{x}) = \frac{1}{|S(\boldsymbol{x}, r)|} \int_{S(\boldsymbol{x},r)} f(\boldsymbol{z})\, d\boldsymbol{\nu}.$$

The authors of [JSW05b] also introduced an elegant continuous version of the the mean value coordinates. Below we give a simple derivation of the continuous mean value coordinates.

Consider the unit sphere $\mathbb{S} = S(\boldsymbol{x}, 1)$ centered at $\boldsymbol{x}$ and parameterized by the outer unit normal $\boldsymbol{\nu}$ (see Fig. 1(a) for a visual feedback on some notations used below). Let $\boldsymbol{y}$ be a point on $\partial\Omega$ and $\rho = |\boldsymbol{x}-\boldsymbol{y}|$. Denote by $\boldsymbol{z}$ the intersection point between the ray $[\boldsymbol{xy})$ and $\mathbb{S}$. Assume that we know the values of function $f(\cdot)$ on $\partial\Omega$ and at $\boldsymbol{x}$. Then we can estimate $f(\boldsymbol{z})$ using the linear interpolation:

$$f(\boldsymbol{z}) \approx \frac{(\rho-1)f(\boldsymbol{x}) + f(\boldsymbol{y})}{\rho}$$

Now let us apply $\mathbb{S}$-averaging to the left and right sides of the above equation:

$$\int_{\mathbb{S}} f(\boldsymbol{z})\, d\boldsymbol{\nu} = |\mathbb{S}|\, f(\boldsymbol{x}) - f(\boldsymbol{x}) \int_{\mathbb{S}} \frac{d\boldsymbol{\nu}}{|\boldsymbol{x}-\boldsymbol{y}|} + \int_{\mathbb{S}} \frac{f(\boldsymbol{y})\, d\boldsymbol{\nu}}{|\boldsymbol{x}-\boldsymbol{y}|}$$

and, assuming that $f(\cdot)$ is harmonic, we arrive at the transfinite mean value interpolation scheme of [JSW05b]

$$f(\boldsymbol{x}) = \int_{\mathbb{S}} \frac{f(\boldsymbol{y})}{|\boldsymbol{x}-\boldsymbol{y}|}\, d\boldsymbol{\nu} \Big/ \int_{\mathbb{S}} \frac{d\boldsymbol{\nu}}{|\boldsymbol{x}-\boldsymbol{y}|}. \qquad (5)$$

This interpolation construction has a natural generalization

$$f(\boldsymbol{x}) = \int_{\mathbb{S}} \frac{f(\boldsymbol{y}) w(\boldsymbol{x}, \boldsymbol{\nu})}{|\boldsymbol{x}-\boldsymbol{y}|}\, d\boldsymbol{\nu} \Big/ \int_{\mathbb{S}} \frac{w(\boldsymbol{x}, \boldsymbol{\nu})}{|\boldsymbol{x}-\boldsymbol{y}|}\, d\boldsymbol{\nu}, \qquad (6)$$

where $w(\boldsymbol{x}, \boldsymbol{\nu})$ is a weighting function associated with interpolated location $\boldsymbol{x}$.

Obviously (6) is just another form of (4) whose kernel satisfies the partition of unity property (2). One can also consider (6) as a transfinite version of the basic Shepard interpolation [She68].

Let us check whether (6) satisfies the linear precision property. For $f(\boldsymbol{x}) \equiv \boldsymbol{x}$ we have $f(\boldsymbol{y}) \equiv \boldsymbol{y} = \boldsymbol{x} + \rho\boldsymbol{\nu}$. Substituting the latter into (6) gives

$$0 = \int_{\mathbb{S}} \boldsymbol{\nu}\, w(\boldsymbol{x}, \boldsymbol{\nu})\, d\boldsymbol{\nu} \quad \text{for each} \quad \boldsymbol{x} \in \Omega \qquad (7)$$

which is necessary and sufficient for linear precision.

One can see that (7) is satisfied if the weighting function is centrally-symmetric, i.e., coincides at each pair of antipodal points:

$$w(\boldsymbol{x}, \boldsymbol{\nu}) = w(\boldsymbol{x}, -\boldsymbol{\nu}). \qquad (8)$$

Consider an important case of the planar interpolation: $n = 2$, $\boldsymbol{\nu} = (\cos\theta, \sin\theta)$,

$$f(\boldsymbol{x}) = \int_0^{2\pi} \frac{f(\boldsymbol{y}) w(\boldsymbol{x}, \theta)}{|\boldsymbol{x}-\boldsymbol{y}|}\, d\theta \Big/ \int_0^{2\pi} \frac{w(\boldsymbol{x}, \theta)}{|\boldsymbol{x}-\boldsymbol{y}|}\, d\theta. \qquad (9)$$

The orthogonality conditions

$$\int_0^{2\pi} w(\boldsymbol{x}, \theta) \cos\theta\, d\theta = 0 = \int_0^{2\pi} w(\boldsymbol{x}, \theta) \sin\theta\, d\theta \qquad (10)$$

for each $\boldsymbol{x} \in \Omega$ are necessary and sufficient for linear precision.

It turns out that any barycentric interpolation scheme can be represented in the form of (6) with the weight function (which may be a measure of a generalized function) satisfying orthogonality conditions (7). Indeed, according to the Riesz representation theorem, given $\boldsymbol{x} \in \Omega$, a linear transfinite interpolation scheme can be considered as a linear functional $T_{\boldsymbol{x}}$ defined on an appropriate space of functions on $\partial\Omega$

$$T_{\boldsymbol{x}} : f|_{\partial\Omega} \to f(\boldsymbol{x})$$

and, therefore, can be represented by integration against a certain density μ_x

$$f(\boldsymbol{x}) \equiv T_x(f) = \int_{\partial\Omega} f(\boldsymbol{y})\mu_x(\boldsymbol{y})\, ds_y. \qquad (11)$$

Denote by $h(\boldsymbol{x},\boldsymbol{y})$ the distance from $\boldsymbol{x}$ to the supporting plane at $\boldsymbol{y}\in\partial\Omega$, as seen in Fig. 1. The area (length) element ds_y of $\partial\Omega$ at $\boldsymbol{y}\in\partial\Omega$ can be expressed in polar coordinates $(\rho,\boldsymbol{\nu})$ centered at $\boldsymbol{x}\in\Omega$ as

$$ds_y = \rho^n d\boldsymbol{\nu}/h. \qquad (12)$$

Therefore we can rewrite (11) as follows

$$T_x(f) = \int_{\mathbb{S}} f(\boldsymbol{y})\mu_x(\boldsymbol{y})\frac{|\boldsymbol{x}-\boldsymbol{y}|^n}{h(\boldsymbol{x},\boldsymbol{y})}\, d\boldsymbol{\nu}.$$

It remains to set $w(\boldsymbol{x},\boldsymbol{\nu}) = \mu_x(\boldsymbol{y})|\boldsymbol{x}-\boldsymbol{y}|^{n+1}/h(\boldsymbol{x},\boldsymbol{y})$.

Below we consider two important examples.

Transfinite Laplace coordinates. The transfinite Laplace coordinates are a continuous version of the discrete harmonic coordinates which are used widely in computational mechanics [SM06]. The discrete Laplace interpolation scheme was probably first time proposed in [CFL82] and then reinvented many times in connection with research on finite element methods [BVIK*97] (the so-called non-Sibsonian interpolation), computational geometry [Sug99], and discrete minimal surfaces [PP99] (the so-called cotangent weights). A particular case of 2D transfinite Laplace coordinates was studied in [HS00] where interpolation of data defined on straight line segments was considered.

Following [SJW06] one can define the transfinite Laplace coordinates in a way similar to the derivation of the transfinite mean value coordinates if, instead of satisfying the mean value property, we search for a solution minimizing the Dirichlet energy. Let us assume that $f(\boldsymbol{x})$ is known and consider a ruled surface patch generated by straight segments connecting inner point $(\boldsymbol{x}, f(\boldsymbol{x}))$, $\boldsymbol{x}\in\Omega$, with all boundary points $(\boldsymbol{y}, f(\boldsymbol{y}))$, $\boldsymbol{y}\in\partial\Omega$. Then $f(\boldsymbol{x})$ is defined such that the Dirichlet energy attains its minimal value.

Let $r=\rho(\theta)\equiv|\boldsymbol{x}-\boldsymbol{y}|$ be the graph of $\partial\Omega$ in the polar coordinates (r,θ) centered at $\boldsymbol{x}$. Denote by $F_{\boldsymbol{x}}(\boldsymbol{z})$, $\boldsymbol{z}\in\Omega$, the ruled surface described in the previous paragraph

$$F_{\boldsymbol{x}}(\boldsymbol{z}) = \frac{(\rho-r)f(\boldsymbol{x}) + rf(\boldsymbol{y})}{\rho}.$$

Here $r=|\boldsymbol{x}-\boldsymbol{z}|$ and $\boldsymbol{y}\in\partial\Omega$ is the intersection point between $\partial\Omega$ and the ray from $\boldsymbol{x}$ through $\boldsymbol{z}$. We arrive at the following minimization problem

$$\min \leftarrow \iint_\Omega |\nabla F_{\boldsymbol{x}}|^2\, d\boldsymbol{z} = \int_0^{2\pi} d\theta \int_0^{\rho} r\, dr \left\{ \left[\frac{f(\boldsymbol{x})-f(\boldsymbol{y})}{\rho}\right]^2 + \right.$$

$$\left. + \left[(f(\boldsymbol{y})-f(\boldsymbol{x}))\left(\frac{1}{\rho}\right)'_\theta + \frac{1}{\rho}f'_\theta(\boldsymbol{y})\right]^2 \right\} =$$

$$= \frac{1}{2}\int_0^{2\pi} d\theta \left\{ [f(\boldsymbol{x})-f(\boldsymbol{y})]^2 + \left[f'_\theta(\boldsymbol{y}) + (f(\boldsymbol{y})-f(\boldsymbol{x}))\frac{\rho'_\theta}{\rho}\right]^2 \right\},$$

where the last integral is a quadratic function w.r.t. $f(\boldsymbol{x})$. Thus the optimal value of $f(\boldsymbol{x})$ is given by

$$f(\boldsymbol{x}) = \frac{\int_0^{2\pi}\left\{f(\boldsymbol{y}) - f'_\theta(\boldsymbol{y})\left[\rho'_\theta/\rho\right] + f(\boldsymbol{y})\left[\rho'_\theta/\rho\right]^2\right\} d\theta}{\int_0^{2\pi}\left\{1+\left[\rho'_\theta/\rho\right]^2\right\} d\theta}$$

$$= \int_0^{2\pi} f(\boldsymbol{y})\frac{\rho''_{\theta\theta}+\rho}{\rho}\, d\theta \Big/ \int_0^{2\pi}\frac{\rho''_{\theta\theta}+\rho}{\rho}\, d\theta, \qquad (13)$$

where integrations by parts are used to derive (13).

Notice that (13) corresponds to (9) with

$$w(\boldsymbol{x},\theta) = \rho''_{\theta\theta} + \rho. \qquad (14)$$

A simple integration by parts shows that (14) satisfies the orthogonality conditions (10).

Probably the simplest way to define the transfinite Laplace coordinates in $\mathbb{R}^n$, $n\geq 3$, consists of expressing the coordinates via the gradient of area (volume), see [MBLD02, DMA02], for the relation between the discrete harmonic coordinates and the gradient of an area functional. Let $\boldsymbol{n}(\boldsymbol{y})$ be the unit outer normal of $\partial\Omega$ at $\boldsymbol{y}\in\partial\Omega$. Denote by $V(\boldsymbol{x})$ the volume of Ω as a function of $\boldsymbol{x}$. Then, similar to the discrete case, we have

$$0 = \nabla_x V(\boldsymbol{x}) = \int_{\partial\Omega} \boldsymbol{n}(\boldsymbol{y})\, ds_y \equiv \int_{\mathbb{S}} \frac{\boldsymbol{n}\, d\boldsymbol{n}}{K(\boldsymbol{n})},$$

where $K(\boldsymbol{n})$ is the Gaussian curvature of $\partial\Omega$ parameterized by its unit normal. Thus, assuming that $\partial\Omega$ is parameterized by its Gauss map, the transfinite Laplace coordinates are given by (6) with

$$w(x,\boldsymbol{\nu}) = 1/K(\boldsymbol{\nu}), \qquad (15)$$

where $K(\boldsymbol{\nu})$ is the Gaussian curvature of $\partial\Omega$ at the point with normal $\boldsymbol{\nu}$.

In 2D, (15) is obviously reduced to (14) (see also Section 6).

Transfinite Wachspress-Warren coordinates. Motivated by FEM applications, Wachspress [Wac75] proposed a construction of affine-invariant barycentric coordinates for convex polygons in 2D. Recently Warren and co-workers [War96, WSHD06] extended the Wachspress coordinates to convex polyhedra in $\mathbb{R}^n$ and presented a transfinite version of the coordinates

Let us denote by $\boldsymbol{n}(\boldsymbol{y})$ the outer unit normal to Ω at $\boldsymbol{y}\in\partial\Omega$. The transfinite Wachspress-Warren coordinates are given by [WSHD06]

$$f(\boldsymbol{x}) = \int_\Omega f(\boldsymbol{y})\frac{K(\boldsymbol{y})\rho(\boldsymbol{x},\boldsymbol{y})}{h(\boldsymbol{x},\boldsymbol{y})^n}\, ds_y \Big/ \int_\Omega \frac{K(\boldsymbol{y})\rho(\boldsymbol{x},\boldsymbol{y})}{h(\boldsymbol{x},\boldsymbol{y})^n}\, ds_y,$$

where $K(\boldsymbol{y})$ is the Gaussian curvature of $\partial\Omega$ at $\boldsymbol{y}$ and, as before, $h(\boldsymbol{x},\boldsymbol{y})$ is the distance from $\boldsymbol{x}$ to the supporting plane at $\boldsymbol{y}\in\partial\Omega$.

Thus, in view of (12), the transfinite Wachspress-Warren coordinates are given by (6) with

$$w(\boldsymbol{x},\boldsymbol{\nu}) = K(\boldsymbol{y})\,[\rho(\boldsymbol{x},\boldsymbol{y})/\,h(\boldsymbol{x},\boldsymbol{y})]^{n+1}\,. \qquad (16)$$

In 2D, straightforward computations show that (16) can be written as

$$w(\boldsymbol{x},\theta) = (1/\rho)''_{\theta\theta} + 1/\rho. \qquad (17)$$

A geometric proof of (17) is given in Section 6. Similar to (14), orthogonality conditions (10) for (17) are easily derived via integration by parts.

Notice a similarity between (17) and (14). It will be explained in Section 6.

3. Pseudo-harmonic interpolation

Let us call an transfinite interpolation scheme *pseudo-harmonic* if it reproduces the harmonic functions in a ball.

Surprisingly, transfinite mean value interpolation (5) does not approximate harmonic functions. Indeed, let us consider the following pseudo-harmonic interpolation scheme

$$f(\boldsymbol{x}) = \int_{\partial\Omega}\frac{f(\boldsymbol{y})\,ds_{\boldsymbol{y}}}{|\boldsymbol{x}-\boldsymbol{y}|^n}\Big/\int_{\partial\Omega}\frac{ds_{\boldsymbol{y}}}{|\boldsymbol{x}-\boldsymbol{y}|^n} \qquad (18)$$

which was introduced for $d=2$ in [CMS98] as a transfinite version of a variant of the well known Shepard interpolation method [She68]

$$f(\boldsymbol{x}) = \frac{\sum_{i=1}^N f(\boldsymbol{y}_i)|\boldsymbol{x}-\boldsymbol{y}_i|^{-n}}{\sum_{i=1}^N |\boldsymbol{x}-\boldsymbol{y}_i|^{-n}}.$$

It is easy to see that (18) coincides with the Poisson Integral Formula for the Laplace equation when Ω is a ball.

According to (12) we can rewrite (18) as follows

$$f(\boldsymbol{x}) = \int_{\mathbb{S}}\frac{f(\boldsymbol{y})\,d\boldsymbol{\nu}}{h(\boldsymbol{x},\boldsymbol{y})}\Big/\int_{\mathbb{S}}\frac{d\boldsymbol{\nu}}{h(\boldsymbol{x},\boldsymbol{y})} \qquad (19)$$

which is another, quite elegant, form of the Poisson Integral Formula. †

In general, (19) (or, equivalently, (18)) does not give linear precision.

It is interesting to observe a similarity and difference between (19) and transfinite mean value coordinates (5). It also explains why (5) does not enjoy the property of being pseudo-harmonic.

Simple computations show that already in 2D the transfinite Laplace coordinates are not pseudo-harmonic. This is not surprising since in general the discrete harmonic coordinates lead to only zeroth-order consistency of the corresponding finite difference approximation of the Laplacian [Suk03]. However the discrete harmonic coordinates deliver a good approximation of the Laplace operator in Sobolev spaces of negative order [War05].

As shown in [FHK06], the discrete harmonic and Wachspress coordinates are the same for a circumscribable polygon. This implies that their transfinite versions coincide for a 2D circle. Thus the transfinite Wachspress-Warren coordinates are not pseudo-harmonic as well.

4. Weighted Gordon-Wixom coordinates

For 2D convex shapes, a simple and elegant construction for transfinite pseudo-harmonic barycentric coordinates was proposed by Gordon and Wixom in [GW74]. Below we describe their multidimensional analog.

Given a point $\boldsymbol{x}$ inside Ω, consider the unit sphere $\mathbb{S}$ centered at $\boldsymbol{x}$ and a unit normal $\boldsymbol{\nu}\in\mathbb{S}$. Let the straight line through $\boldsymbol{x}$ determined by $\boldsymbol{\nu}$ intersect the boundary $\partial\Omega$ in two points $\boldsymbol{y}_1$ and $\boldsymbol{y}_2$. Denote by ρ_1 and ρ_2 the distances from $\boldsymbol{x}$ to $\boldsymbol{y}_1$ and $\boldsymbol{y}_2$, respectively. Now we estimate $f(\boldsymbol{x})$ using the linear interpolation between $f(\boldsymbol{y}_1)$ and $f(\boldsymbol{y}_2)$

$$f(\boldsymbol{x},\theta) = \frac{\rho_2}{\rho_1+\rho_2}f(\boldsymbol{y}_1) + \frac{\rho_1}{\rho_1+\rho_2}f(\boldsymbol{y}_2) = \qquad (20)$$
$$= \left[\frac{f(\boldsymbol{y}_1)}{\rho_1}+\frac{f(\boldsymbol{y}_2)}{\rho_2}\right]\Big/\left[\frac{1}{\rho_1}+\frac{1}{\rho_2}\right]$$

$\mathbb{S}$-averaging w.r.t. $\boldsymbol{\nu}$ defines the Gordon-Wixom interpolation

$$f(\boldsymbol{x}) = \frac{1}{|\mathbb{S}|}\int_{\mathbb{S}}\left[\frac{\rho_2}{\rho_1+\rho_2}f(\boldsymbol{y}_1)+\frac{\rho_1}{\rho_1+\rho_2}f(\boldsymbol{y}_2)\right]d\boldsymbol{\nu}. \qquad (21)$$

As shown below for a more general situation, the Gordon-Wixom interpolation scheme is pseudo-harmonic and has linear precision.

Similar to weighted transfinite mean value coordinates (6), let us introduce a weighted version of the Gordon-Wixom interpolation scheme

$$f(\boldsymbol{x}) = \frac{\int_{\mathbb{S}}\left[\left(\frac{f(\boldsymbol{y}_1)}{\rho_1}+\frac{f(\boldsymbol{y}_2)}{\rho_2}\right)\Big/\left(\frac{1}{\rho_1}+\frac{1}{\rho_2}\right)\right]W(\boldsymbol{x},\boldsymbol{\nu})\,d\boldsymbol{\nu}}{\int_{\mathbb{S}}W(\boldsymbol{x},\boldsymbol{\nu})\,d\boldsymbol{\nu}}, \qquad (22)$$

where $W(\boldsymbol{x},\boldsymbol{\nu})$ is centrally-symmetric (8).

† Certainly representations (18) and (19) of the solution to the Laplace equation in a ball are deserved to be mentioned in PDE textbooks.

To show that (22) enjoys linear precision let us set $f(\boldsymbol{x}) \equiv \boldsymbol{x}$. Then $f(\boldsymbol{y}_1) \equiv \boldsymbol{y}_1 = \boldsymbol{x} + \rho_1\boldsymbol{\nu}$ and $f(\boldsymbol{y}_2) \equiv \boldsymbol{y}_2 = \boldsymbol{x} - \rho_2\boldsymbol{\nu}$ and (22) is obviously satisfied.

Observe that if weighting function of (6) satisfies (8) (centrally-symmetric), then the weighting functions of (22) and (6) are related to each other by

$$W(\boldsymbol{x},\boldsymbol{\nu}) = w(\boldsymbol{x},\boldsymbol{\nu})\left(\frac{1}{\rho_1}+\frac{1}{\rho_2}\right).$$

In particular, (22) with $W(\boldsymbol{x},\boldsymbol{\nu}) = 1/\rho_1 + 1/\rho_2$ is reduced to mean value coordinates (5).

Now let us consider a particular case of (22) obtained when $W(\boldsymbol{x},\boldsymbol{\nu})$ depends on distances ρ_1 and ρ_2 only. Since $W(\boldsymbol{x},\boldsymbol{\nu})$ is centrally-symmetric, it can be written as a function of $\rho_1 \cdot \rho_2$ and $\rho_1 + \rho_2$

$$W(\boldsymbol{x},\boldsymbol{\nu}) = W(\rho_1+\rho_2, \rho_1\rho_2). \tag{23}$$

Let us show that if (23) depends only on the product of ρ_1 and ρ_1, then barycentric coordinates (22) are pseudo-harmonic. Indeed if Ω is a ball then according to the Intersecting Chords Theorem [‡]

$$\rho_1\rho_2 \equiv c(\boldsymbol{x}),$$

where $c(\boldsymbol{x})$ depends only on $\boldsymbol{x}$. Thus it is sufficient to demonstrate that (21) is pseudo-harmonic. Notice that we can exploit symmetry properties of (21) and rewrite it as

$$f(\boldsymbol{x}) = \frac{2}{|\mathbb{S}|}\int_{\mathbb{S}/2}\frac{\rho_2}{\rho_1+\rho_2}f(\boldsymbol{y}_1)\,d\boldsymbol{\nu}, \tag{24}$$

where by $\mathbb{S}/2$ we denote a unit semisphere. Let Ω be a ball of radius R. Consider the 2D disc obtained as the intersection between Ω and the plane formed by $\boldsymbol{y}_1$, $\boldsymbol{y}_2$, and the center of the ball. In notations of Fig. 1(b), we obviously have

$$h_1 = \rho_1\sin\varphi, \quad h_2 = \rho_2\sin\varphi, \quad \rho_1+\rho_2 = 2R\sin\varphi,$$
$$\frac{h_1h_2}{\sin^2\varphi} = c(\boldsymbol{x}), \quad \frac{\rho_2}{\rho_1+\rho_2} = \frac{h_2}{2R\sin^2\varphi} = \frac{c(\boldsymbol{x})}{2R}\cdot\frac{1}{h_1}.$$

Thus (24) is reduced to (19). A slightly more complex proof of this result for the 2D version of (21) is given in [GW74] and attributed to W. W. Meyer.

Now we can see why the original Gordon-Wixom interpolation scheme is good in approximating harmonic functions. The second-order directional derivative of $f(\boldsymbol{x})$ in the $\boldsymbol{\nu}$-direction can be approximated by

$$f''_{\boldsymbol{\nu}\boldsymbol{\nu}}(\boldsymbol{x}) \approx D_{\boldsymbol{\nu}\boldsymbol{\nu}}[f(\boldsymbol{x})] \equiv \tag{25}$$
$$\equiv \frac{2}{\rho_1\rho_2}\left(\left[\frac{f(\boldsymbol{y}_1)}{\rho_1}+\frac{f(\boldsymbol{y}_2)}{\rho_2}\right]\Big/\left[\frac{1}{\rho_1}+\frac{1}{\rho_2}\right]-2f(\boldsymbol{x})\right).$$

[‡] The Intersecting Chords Theorem is usually formulated for a 2D circle. However its extension onto the multidimensional case is straightforward.

Since

$$2\Delta f(\boldsymbol{x}) = \frac{1}{|\mathbb{S}|}\int_{\mathbb{S}} f''_{\boldsymbol{\nu}\boldsymbol{\nu}}(\boldsymbol{x})\,d\boldsymbol{\nu},$$

we obtain weighted Gordon-Wixom interpolation (22) with weight

$$W(\boldsymbol{x},\boldsymbol{\nu}) = \frac{1}{\rho_1\rho_2} \tag{26}$$

and, according to the Intersecting Chords Theorem, arrive at (21) when Ω is a ball.

As mentioned before, weighting functions $w(\boldsymbol{x},\boldsymbol{\nu})$ in (6) and $W(\boldsymbol{x},\boldsymbol{\nu})$ in (22) may be generalized functions. In particular, Gordon and Wixom [GW74] considered a transfinite interpolation scheme which can be obtained from (22) if we set $W(\boldsymbol{x},\boldsymbol{\nu}) = \delta(\boldsymbol{\nu}-\boldsymbol{\nu}_0)$, where $\delta(\cdot)$ is the Dirac delta function and $\boldsymbol{\nu}_0$ is a given direction.

Non-convex domains. So far we have assumed that Ω is convex. It turns out that it is very easy to extend the weighted Gordon-Wixom interpolation scheme (22) to generic non-convex domains. Consider the straight line $l(\boldsymbol{x},\boldsymbol{\nu})$ through $\boldsymbol{x}$ at direction $\boldsymbol{\nu}$ intersecting $\partial\Omega$ in m points $\boldsymbol{y}_1,\ldots,\boldsymbol{y}_m$. Let us set $\varepsilon_i = 1$ if the ray $[\boldsymbol{x},\boldsymbol{y}_i)$ arrives at $\boldsymbol{y}_i$ from inside of Ω, $\varepsilon_i = -1$ if the ray approaches $\boldsymbol{y}_i$ from outside of Ω, and $\varepsilon_i = 0$ if the ray is tangent to $\partial\Omega$ at $\boldsymbol{y}_i$. Define

$$f(\boldsymbol{x},\boldsymbol{\nu}) = \sum_{i=1}^{m} f(\boldsymbol{y}_i)w(\boldsymbol{x},\boldsymbol{y}_i)\frac{\varepsilon_i}{\rho_i}\Big/\sum_{i=1}^{m} w(\boldsymbol{x},\boldsymbol{y}_i)\frac{\varepsilon_i}{\rho_i}, \tag{27}$$

where $\rho_i = |\boldsymbol{x}-\boldsymbol{y}_i|$. This simple one-dimensional construction belongs to the family of barycentric rational interpolation schemes studied widely in constructive approximation [BBM05]. Now $\mathbb{S}$-averaging w.r.t. $\boldsymbol{\nu}$

$$f(\boldsymbol{x}) = \frac{1}{|\mathbb{S}|}\int_{\mathbb{S}} f(\boldsymbol{x},\boldsymbol{\nu})\,d\boldsymbol{\nu} \tag{28}$$

gives an extension of (22) to generic non-convex domains.

If Ω is not generic, it may happen that $l(\boldsymbol{x},\boldsymbol{\nu})\cap\partial\Omega$ contains linear segments. It is natural to treat such a situation as the tangency case and set $\varepsilon = 0$ in (27) for all the points of those linear segments on $l(\boldsymbol{x},\boldsymbol{\nu})$.

Instead of (27) one can use high-order 1D barycentric interpolation schemes introduced very recently by Floater and Hormann [FH06].

An example of interpolating inside of a non-convex polygon with (27) is shown in Fig.1(c). Similar to [GW74] we evaluate (28) numerically.

Gordon-Wixom coordinates for polygons. Let Ω be a 2D convex polygon and $f(\boldsymbol{y})$, $\boldsymbol{y}\in\partial\Omega$, be given by its values at the polygon vertices. Assume that $f(\boldsymbol{y})$ is linear on the edges of the polygon. Then (21) allows

for a closed-form solution. For a planar domain, one can rewrite (21) as

$$\frac{1}{\pi}\int_0^{2\pi}\frac{\rho_2}{\rho_1+\rho_2}f(\boldsymbol{y}_1)\,d\theta. \tag{29}$$

Consider point $\boldsymbol{x}$ inside polygon Ω and place new vertices on the boundary of the polygon such that the straight line connecting x with an original vertex intersects $\partial\Omega$ in another, possibly new, vertex. See Fig. 1(d) where A and D are original polygon vertices and B and C are new vertices. Then we repeat trigonometric calculations of [Flo03] and, in the notations of Fig. 1(d), arrive at

$$\rho_1(\theta)=\frac{ab\sin\alpha}{a\sin\theta+b\sin(\alpha-\theta)},$$

$$\lambda_1=\frac{b\sin(\alpha-\theta)}{a\sin\theta+b\sin(\alpha-\theta)},\quad \lambda_2=\frac{a\sin(\theta)}{a\sin\theta+b\sin(\alpha-\theta)},$$

where $\lambda_1(\theta)$ and $\lambda_2(\theta)$, $\lambda_1+\lambda_2=1$, are the weights for the linear interpolation inside the segment AB. We compute $\rho_2(\theta)$ in a similar way and get the following formula for the part of (29) corresponding to AB.

$$\frac{1}{\pi}\int_0^{\alpha}\frac{cd\,[f(A)b\sin(\alpha-\theta)+f(B)a\sin\theta]}{ac(b+d)\sin\theta+bd(a+c)\sin(\alpha-\theta)}\,d\theta. \tag{30}$$

Although (30) looks quite complex, it can be evaluated in closed form (we have used Maple to express (30) in terms of elementary functions). Unfortunately the result is too lengthy to present here.

5. Barycentric coordinates and PDEs

Quasi-Laplacian. Let us consider the Dirichlet boundary value problem for a quasi-Laplacian operator:

$$\nabla\cdot(a(\boldsymbol{x})\nabla f(\boldsymbol{x}))=0 \text{ in } \Omega,\quad f(\boldsymbol{x}) \text{ is known on } \partial\Omega, \tag{31}$$

where $a(\boldsymbol{x})>0$ is a known conductivity coefficient. Integration by parts gives

$$\int_{S(\boldsymbol{x},r)} a\frac{\partial f}{\partial\boldsymbol{\nu}}\,d\boldsymbol{\nu}=0, \tag{32}$$

where, as before, $S(\boldsymbol{x},r)$ is the sphere of radius r centered at $\boldsymbol{x}$ and contained inside Ω and $\boldsymbol{\nu}$ is outward unit normal to $S(\boldsymbol{x},r)$. Let us group opposite points of $\mathbb{S}_r$ together in (32):

$$a\frac{\partial f}{\partial\boldsymbol{\nu}}\Big|_{x+r(\boldsymbol{\nu})}-a\frac{\partial f}{\partial\boldsymbol{\nu}}\Big|_{x-r(\boldsymbol{\nu})}\approx 2r\frac{\partial}{\partial\boldsymbol{\nu}}\left(a(\boldsymbol{x})\frac{\partial f(\boldsymbol{x})}{\partial\boldsymbol{\nu}}\right)=$$
$$=2r\left[a'_{\boldsymbol{\nu}}(\boldsymbol{x})f'_{\boldsymbol{\nu}}+a(\boldsymbol{x})f''_{\boldsymbol{\nu}\boldsymbol{\nu}}\right] \tag{33}$$

We estimate the first- and second-order directional derivatives of $f(\cdot)$ by

$$f'_{\boldsymbol{\nu}}(\boldsymbol{x})\approx\frac{f(\boldsymbol{y}_1)-f(\boldsymbol{x})}{\rho_1},$$

and (25), respectively. Substituting these approximations into the right hand-side of (33), integrating over a half-sphere $S(\boldsymbol{x},r)/2$, and taking into account (32) yields

$$0\approx\int_{\mathbb{S}/2}\frac{f(\boldsymbol{y}_1)-f(\boldsymbol{x})}{\rho_1}a'_{\boldsymbol{\nu}}(\boldsymbol{x})\,d\boldsymbol{\nu}+a(\boldsymbol{x})\int_{\mathbb{S}/2}D_{\boldsymbol{\nu}\boldsymbol{\nu}}[f(\boldsymbol{x})]\,d\boldsymbol{\nu} \tag{34}$$

with $D_{\boldsymbol{\nu}\boldsymbol{\nu}}[f(\boldsymbol{x})]$ defined in (25). We rewrite the integrals in the right-hand side of (34) as integrals over the whole unit sphere $\mathbb{S}$ and arrive at

$$f(\boldsymbol{x})\left[\int_{\mathbb{S}}\frac{a'_{\boldsymbol{\nu}}(\boldsymbol{x})}{\rho}\,d\boldsymbol{\nu}+2a(\boldsymbol{x})\,|\mathbb{S}|\right]\approx$$
$$\approx\int_{\mathbb{S}}\frac{f(\boldsymbol{y})}{\rho}\,a'_{\boldsymbol{\nu}}(\boldsymbol{x})\,d\boldsymbol{\nu}+a(\boldsymbol{x})\int_{\mathbb{S}}D_{\boldsymbol{\nu}\boldsymbol{\nu}}[f(\boldsymbol{x})]\,d\boldsymbol{\nu}$$

which can be considered as a combination of the (26)-weighted Gordon-Wixom interpolation scheme and $a'_{\boldsymbol{\nu}}(x)$-weighted transfinite mean value coordinates.

Note that it does not satisfy the linear precision property because of weighting function $a'_{\boldsymbol{\nu}}(x)$ in the mean value component. Notice however that linear functions do not satisfy (31) unless the conductivity coefficient $a(\boldsymbol{x})$ is constant.

Of course, linear PDE (31) is rather a toy example. However a similar approximation approach can be applied to quasi-linear PDE operators in the form

$$\frac{2}{|\mathbb{S}|}\int_{\mathbb{S}/2}\partial_{\boldsymbol{\nu}}\left(g\left(|\partial_{\boldsymbol{\nu}}f|\right)\partial_{\boldsymbol{\nu}}f\right)\,d\boldsymbol{\nu}, \tag{35}$$

where $g(\cdot)$ is a positive function. A 2D version of (35) was used in [Wei94] for anisotropic nonlinear image diffusion purposes.

AMLE. According to an axiomatic approach to image interpolation developed in [CMS98] and numerical experiments conducted in [ACGR02], absolutely minimizing functions [ACJ04] satisfy many properties desirable for a feature-preserving interpolation of height data.

Weighted Gordon-Wixom coordinates (21) approximate the solution to the AMLE equation if we set $W(\boldsymbol{x},\boldsymbol{\nu})=\delta(\boldsymbol{\nu}-\boldsymbol{\nu}_0(\boldsymbol{x}))$, where $\boldsymbol{\nu}_0(\boldsymbol{x})$ is a direction for which the right-hand side of

$$f'_{\boldsymbol{\nu}}(\boldsymbol{x})\approx\frac{f(\boldsymbol{y}_1)-f(\boldsymbol{y}_2)}{\rho_1+\rho_2}, \tag{36}$$

attains its maximal absolute value. Similar to the AMLE interpolation, (36) is capable of interpolating isolated values. For example, let Ω be the unit disk without its center (a punctured disk). Define $f(\boldsymbol{y})=1$ at the disk center and $f(\boldsymbol{y})\equiv 0$ on the outer boundary of the punctured disk. Then the solution to (36) is given by cone $f(\boldsymbol{x})=1-|\boldsymbol{x}|$. Exactly the same result is delivered by AMLE.

6. Christoffel-Minkowski type problems and barycentric coordinates

So far we have studied abilities of various barycentric interpolation schemes to approximate solutions to second-order elliptic PDEs. In this section, we reveal and discuss surprising links between the barycentric coordinates and classical inverse problems of differential and convex geometry.

Minkowski problem. The classical Minkowski problem is an inverse problem in differential geometry and concerns reconstruction of a closed convex hypersurface from its Gaussian curvature given as a function of the outer surface normal [Min03]. Given a positive function $K(\boldsymbol{\nu})$ defined over the unit sphere $\mathbb{S}$, a necessary and sufficient condition of the Minkowski problem is

$$\int_{\Sigma} \boldsymbol{\nu}\, dl \equiv \int_{\mathbb{S}} \frac{\boldsymbol{\nu}\, d\boldsymbol{\nu}}{K(\boldsymbol{\nu})} = 0, \tag{37}$$

where Σ is the reconstructed hypersurface, dl its area element and $dl = K\, d\boldsymbol{\nu}$ by definition of the Gaussian curvature. The necessity of (37) follows immediately from the divergence theorem of vector calculus. The sufficiency is non-trivial and was proven, under various assumptions of smoothness of Σ, by Minkowski himself (1903), Alexandrov (1938), Lewy (1938), Miranda (1939), Pogorelov (1952), Nirenberg (1953), Cheng and Yau (1976), and others.

Exploring the similarity between (37) and (7), we get for free the following result delivering a geometric description of barycentric interpolation schemes. For each $\boldsymbol{x} \in \Omega$, consider a family of hyperplanes in $\mathbb{R}^n_{\boldsymbol{z}}$

$$(\boldsymbol{z} - \boldsymbol{x}) \cdot \boldsymbol{\nu} = p(\boldsymbol{x}, \boldsymbol{\nu}) \tag{38}$$

parameterized by $\boldsymbol{\nu} \in \mathbb{S}$. For a given $\boldsymbol{\nu}$, $p(\boldsymbol{x}, \boldsymbol{\nu})$ stands for the signed distance from the plane defined by $\boldsymbol{\nu}$ to $\boldsymbol{x}$. We assume that $p(\boldsymbol{x}, \boldsymbol{\nu})$ is sufficiently smooth. Denote by $\Sigma_{\boldsymbol{x}}$ the envelope of family (38) and let $K_{\boldsymbol{x}}(\boldsymbol{\nu})$ be the Gaussian curvature of $\Sigma_{\boldsymbol{x}}$. Assuming that $\Sigma_{\boldsymbol{x}}$ is convex (and, therefore, its Gaussian curvature is positive), we obtain transfinite barycentric coordinates (6) with $w(\boldsymbol{x}, \boldsymbol{\nu}) = 1/K_{\boldsymbol{x}}(\boldsymbol{\nu})$. Vice versa, given barycentric coordinates (6) whose weighting function $w(\boldsymbol{x}, \boldsymbol{\nu})$ is positive at $\boldsymbol{x}$, a convex hypersurface $\Sigma_{\boldsymbol{x}}$ is reconstructed from its Gaussian curvature

$$K_{\boldsymbol{x}}(\boldsymbol{\nu}) = 1/w(\boldsymbol{x}, \boldsymbol{\nu}).$$

In order to use the Minkowski problem for a geometric description of barycentric coordinates (6) whose weighting function $w(\boldsymbol{x}, \boldsymbol{\nu})$ is not always positive, one can consider the so-called hedgehogs, closed surfaces parameterized by their Gauss maps and described as the envelops of their tangent planes. Unfortunately, if $n \geq 3$, (37) is not sufficient in the case of envelopes forming non-convex surfaces [MM01](Proposition 7).

Christoffel-Minkowski problem. A generalization of the Minkowski problem, the so-called Christoffel-Minkowski problem, consists of finding a convex hypersurface Σ with a prescribed elementary symmetric polynomial of the surface principal radii [GG02]. For $\boldsymbol{\lambda} = (\lambda_1, \ldots, \lambda_{n-1}) \in \mathbb{R}^{n-1}$, let $S_k[\boldsymbol{\lambda}]$ be an elementary symmetric polynomial of degree k

$$S_k[\boldsymbol{\lambda}] = \sum_{i_1 < \ldots < i_{n-1}} \lambda_{i_1} \ldots \lambda_{i_{n-1}},$$

where the sum is taken over all permutations of the indices $\{1, \ldots, n-1\}$. Denote by $R_i(\boldsymbol{\nu}) = 1/k_i(\boldsymbol{\nu})$ the surface principal radii parameterized by the Gauss map of the surface. Direct computations (see, for example, [Bla30, BF34, Bus58, Sch93]) show that $R_i(\boldsymbol{\nu})$, $i = 1, \ldots, n-1$, are the eigenvalues of the matrix

$$\nabla^2_{\boldsymbol{\nu}} p(\boldsymbol{\nu}) + p(\boldsymbol{\nu}) I,$$

where $\nabla^2_{\boldsymbol{\nu}}$ is the Hessian operator w.r.t. a local orthonormal frame on $\mathbb{S}$ and I is the identity matrix. It can be shown [BF34, Bus58, Sch93] that

$$\int_{\mathbb{S}} \boldsymbol{\nu} S_k[R_1, \ldots, R_{n-1}](\boldsymbol{\nu})\, d\boldsymbol{\nu} = 0. \tag{39}$$

The Christoffel-Minkowski problem consists of determining a convex surface whose curvature radii $R_1(\boldsymbol{\nu}), \ldots, R_{n-1}(\boldsymbol{\nu})$ satisfy

$$S_k[R_1, \ldots, R_{n-1}](\boldsymbol{\nu}) = \varphi(\boldsymbol{\nu}), \tag{40}$$

where $\varphi(\boldsymbol{\nu})$ is a given function such that

$$\int_{\mathbb{S}} \boldsymbol{\nu} \varphi(\boldsymbol{\nu})\, d\boldsymbol{\nu} = 0. \tag{41}$$

Orthogonality condition (41) generalizes (37) and can be used for a geometric characterization of transfinite barycentric coordinates.

A substantial progress in solving the general Christoffel-Minkowski problem for convex bodies was recently achieved in [GG02, STW04].

The Monge-Ampère equation

$$K(\boldsymbol{\nu}) \equiv \det\left[\nabla^2_{\boldsymbol{\nu}} p(\boldsymbol{\nu}) + p(\boldsymbol{\nu}) I\right] = \varphi(\boldsymbol{\nu})$$

used to solve the Minkowski problem is a particular case of (40) which arises when the product of the curvature radii is considered:

$$S_{n-1}[R_1, \ldots, R_{n-1}] = R_1 \cdot \ldots \cdot R_{n-1} \equiv 1/K.$$

Christoffel problem. Another particular case of the Christoffel-Minkowski problem is obtained from (40) when $k = 1$. It gives the so-called Weingarten formula [Wei84] (as cited in [Bla30])

$$\begin{aligned} &\operatorname{trace}\left[\nabla^2_{\boldsymbol{\nu}} p(\boldsymbol{\nu}) + p(\boldsymbol{\nu}) I\right] \equiv \\ &\equiv \Delta_{\boldsymbol{\nu}} p(\boldsymbol{\nu}) + (n-1) p(\boldsymbol{\nu}) = R(\boldsymbol{\nu}), \end{aligned} \tag{42}$$

where $\Delta_{\boldsymbol{\nu}}$ is the spherical Laplacian and

$$R(\boldsymbol{\nu}) = \sum_{i=1}^{n-1} R_i(\boldsymbol{\nu})$$

is the sum of the principal curvature radii (the reciprocal of the sum is the so-called *harmonic curvature*). Since $\lambda = (n-1)$ is the first eigenvalue of $\Delta_{\boldsymbol{\nu}}$ and $\boldsymbol{\nu}$ are the corresponding $n-1$ eigenfunctions, the necessary and sufficient condition of solvability (42) is given by

$$\int_{\Sigma} \boldsymbol{\nu} R(\boldsymbol{\nu})\, ds = 0. \tag{43}$$

In 3D, this particular case of the Christoffel-Minkowski problem was proposed and studied by Christoffel in 1865 [Chr65] and seems to be the earliest inverse problem in differential and convex geometry. For a relatively recent account, see, for example, [Sch93](Section 4.3),

Given barycentric coordinates (6) with weighting function $w(\boldsymbol{x}, \boldsymbol{\nu})$ satisfying (7), for each $\boldsymbol{x} \in \Omega$ we set

$$R(\boldsymbol{x}, \boldsymbol{\nu}) = w(\boldsymbol{x}, \boldsymbol{\nu})$$

and solve linear second-order elliptic PDE (42) Then surface $\Sigma_{\boldsymbol{x}}$ is reconstructed from support function $p(\boldsymbol{x}, \boldsymbol{\nu})$. (The simplest way to solve (42) consists of expanding $w(\boldsymbol{x}, \boldsymbol{\nu})$ into spherical harmonics and constructing support function $p(\boldsymbol{x}, \boldsymbol{\nu})$ of $\Sigma_{\boldsymbol{\nu}}$ as a spherical harmonic series.)

Christoffel-Minkowski problems in 2D and 3D. In 2D, the Christoffel and Minkowski problems coincide and lead to the following second-order differential equation

$$p''(\theta) + p(\theta) = R(\theta) \equiv 1/k(\theta) \tag{44}$$

for the support function $p(\theta)$. Curve Σ is then obtained from its support function $p(\theta)$ in the following parametric form

$$\boldsymbol{z}(\theta) \equiv \begin{bmatrix} z_1 \\ z_2 \end{bmatrix}(\theta) = \begin{bmatrix} x_1 \\ x_2 \end{bmatrix} + \begin{bmatrix} p(\theta)\cos\theta + p'(\theta)\sin\theta \\ p(\theta)\sin\theta + p'(\theta)\cos\theta \end{bmatrix} \tag{45}$$

For our purposes, for each $\boldsymbol{x} \in \Omega$ we determine $\Sigma_{\boldsymbol{\nu}}$ by solving

$$p''(\theta) + p(\theta) = w(\boldsymbol{x}, \theta) \tag{46}$$

and then using (45). If $w(\boldsymbol{x}, \theta)$ is a positive function of θ, then $\Sigma_{\boldsymbol{x}}$ forms a convex curve. If $w(\boldsymbol{x}, \theta)$ changes its sign, $\Sigma_{\boldsymbol{x}}$ has cusps at the points corresponding to the zeros of the curvature radius $R(\theta) = w(\boldsymbol{x}, \theta)$.

Fig. 2 shows an example of a planar curve generated from its support function.

In 3D, we have two types of the Christoffel-Minkowski problems corresponding to the Gaussian curvature (the Minkowski problem) and harmonic curvature (the Christoffel problem). For the Christoffel problem, $\Sigma_{\boldsymbol{x}}$ is reconstructed by solving

$$\Delta_{\boldsymbol{\nu}} p(\boldsymbol{\nu}) + 2p(\boldsymbol{\nu}) = w(\boldsymbol{x}, \boldsymbol{\nu}). \tag{47}$$

Then one can reconstruct $\Sigma_{\boldsymbol{x}}$ from its support function $p(\boldsymbol{\nu})$ using formulas derived in [VF92]. Similar to the 2D case, $w(\boldsymbol{x}, \boldsymbol{\nu})$ may change its sign and $\Sigma_{\boldsymbol{x}}$ form cuspidal edges at the points where its harmonic curvature $1/w(\boldsymbol{x}, \boldsymbol{\nu})$ becomes infinite.

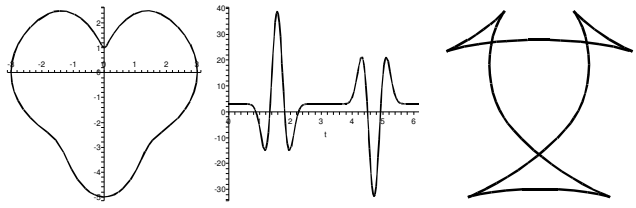

(a) (b) (c)

Figure 2: *(a) Polar plot of a given support function $p(\theta)$. (b) Graph of the curvature radius $R(\theta) = p''(\theta) + p(\theta)$. (c) The curve reconstructed from its support function $p(\theta)$. The curve has six cusps corresponding to the zeros of its curvature radius $R(\theta)$.*

Pedal and negative pedal surfaces. Pedal curves and surfaces are differential geometry objects which have a special significance in classical geometric optics [Her00] and are often mentioned in textbooks on classical differential geometry. Given a surface Σ and a point $\boldsymbol{x}$, the *pedal* of Σ w.r.t. $\boldsymbol{x}$ is defined as the locus of the foots of the perpendiculars from $\boldsymbol{x}$ to the tangent planes to the surface. The negative pedal curves and surfaces are much less mentioned in the differential geometry literature in spite of the fact that they can be used for designing mirrors with prescribed properties [FMR01]. The *negative pedal* of Σ w.r.t. $\boldsymbol{x}$ is constructed as the envelope of planes passing through the points of Σ and perpendicular to the segments connecting $\boldsymbol{x}$ with the points of Σ. The pedal and negative pedal curves and surfaces are also studied in the projective geometry framework [CG67](Chapter 6).

Pedals and negative pedals find applications in materials science [POMZ99]. Following [POMZ99] let us consider two Legendre transformations of positive functions defined on the unit sphere $\mathbb{S}$. Let $r : \mathbb{S} \to \mathbb{R}_+$ be a continuous function. The *polar plot* of $r(\boldsymbol{\nu})$, $\boldsymbol{\nu} \in \mathbb{S}$, is the surface (curve in 2D) defined in the $(r, \boldsymbol{\nu})$ polar coordinates by $r = r(\boldsymbol{\nu})$. The first Legendre transform $r_*(\boldsymbol{\omega})$ is the function corresponding to the negative pedal of the polar plot of $r(\boldsymbol{\nu})$. The second Legendre transform $r^*(\boldsymbol{\nu})$ is the function corresponding to the pedal of the polar plot of $r(\boldsymbol{\omega})$.

As demonstrated in [POMZ99], the following dual-

ity relations are hold

$$1/r^* = [1/r]_*, \quad 1/r_* = [1/r]^*. \tag{48}$$

In addition, if $r(\boldsymbol{\nu})$ satisfies certain convexity conditions, then

$$[r_*]^*(\boldsymbol{\nu}) \equiv r(\boldsymbol{\nu}) \equiv [r^*]_*(\boldsymbol{\nu}). \tag{49}$$

Geometry of Wachspress-Warren coordinates. Now we are ready to establish a link between the transfinite Wachspress-Warren coordinates and the Minkowski problem. As before, given a convex bounded domain Ω in $\mathbb{R}^n$ and point $\boldsymbol{x} \in \Omega$, let $r = \rho(\boldsymbol{\nu})$ be the polar plot of $\partial\Omega$ w.r.t. $\boldsymbol{x}$, $K(\boldsymbol{y})$ denote the Gaussian curvature of $\partial\Omega$ at $\boldsymbol{y} \in \partial\Omega$, and $h(\boldsymbol{x}, \boldsymbol{y}) = (\boldsymbol{y} - \boldsymbol{x}) \cdot \boldsymbol{n}(\boldsymbol{y})$, where $\boldsymbol{n}(\boldsymbol{y})$ is outer unit normal to $\partial\Omega$ at $\boldsymbol{y}$, be the support function of $\partial\Omega$ w.r.t. $\boldsymbol{x}$. Consider surface $\Sigma_{\boldsymbol{x}}$ whose support function w.r.t. $\boldsymbol{x}$ is given by $1/\rho(\boldsymbol{\nu})$. Using duality relations (48) and (49) it is easy to show that the reciprocal of the Gaussian curvature of $\Sigma_{\boldsymbol{x}}$ is given by $K\rho^{n+1}/h^{n+1}$. Thus, according to (37), we have proven the linear precision property of transfinite Wachspress-Warren coordinates (6), (16). In the 2D case, (17) now follows from (44).

An equivalent interpretation of the transfinite Wachspress-Warren coordinates in terms of pedal surfaces (polar duals) was considered in [WSHD06, SJW06] (see also [JSW05a] where a similar description of the discrete Wachspress-Warren coordinates is presented).

Geometry behind Laplace coordinates. According to (15), the geometry of the transfinite Laplace coordinates is simpler than that of Wachspress-Warren coordinates. It is reduced to the Minkowski problem for $\partial\Omega$ (therefore, it can be called by the Minkowski extension of the 2D Laplace coordinates). For each $\boldsymbol{x} \in \Omega$, the support function of $\Sigma_{\boldsymbol{x}}$ is given by $r = \rho(\boldsymbol{\nu})$, the polar plot of $\partial\Omega$ w.r.t. $\boldsymbol{x}$. The linear precision is guaranteed by (37).

It seems, however, that the Christoffel extension of the 2D Laplace coordinates is more appropriate for approximating harmonic functions than the Minkowski extension considered in the previous paragraph. Indeed, let us assume that functions $p(\boldsymbol{\nu})$ and $R(\boldsymbol{\nu})$, $\boldsymbol{\nu} \in \mathbb{S}$, in (43) are defined in $\mathbb{R}^n$ as homogeneous of degree one: $p(t\boldsymbol{z}) \equiv tp(\boldsymbol{z})$ and $R(t\boldsymbol{z}) \equiv tR(\boldsymbol{z})$, $\boldsymbol{z} \in \mathbb{R}^n$. Then (43) can be rewritten as

$$\Delta_{\boldsymbol{z}} p(\boldsymbol{z}) = R(\boldsymbol{z}) \tag{50}$$

and the left-hand side of (50) with $p(\boldsymbol{z}) = \rho(\boldsymbol{z})$, where $\rho(\boldsymbol{\nu})$ is the polar plot of $\partial\Omega$, defines the weighting function

$$w(\boldsymbol{x}, \boldsymbol{\nu}) = R(\boldsymbol{z}/|\boldsymbol{z}|) \tag{51}$$

corresponding to the Christoffel extension of the 2D Laplace coordinates. The Laplacian from the left-hand side of (50) indicates that (6) with (51) is a proper choice for approximating harmonic functions.

Weighted Gordon-Wixom coordinates. As mentioned before, weighted Gordon-Wixom coordinates (22) are equivalent to (6) with centrally-symmetric weighting: $w(\boldsymbol{x}, \boldsymbol{\nu}) = w(\boldsymbol{x}, -\boldsymbol{\nu})$. Therefore, surfaces $\Sigma_{\boldsymbol{x}}$ constructed as solutions to a Christoffel-Minkowski problem are also centrally-symmetric. Centrally-symmetric convex bodies possess interesting properties and are widely studied in convex geometry [BF34, Sch93].

Geometry behind mean value coordinates. Since for the mean value coordinates $\Sigma_{\boldsymbol{x}}$ is always the unit sphere $\mathbb{S}$, these coordinates play a distinguish role in the above inverse problem constructions and correspond to the case when curvature function $S_k[R_1, \ldots, R_{n-1}](\boldsymbol{\nu})$ from (40) is constant.

Algebra of barycentric coordinates. Given two sets defined by their support functions, say $p(\boldsymbol{\nu})$ and $q(\boldsymbol{\nu})$, $\boldsymbol{\nu} \in \mathbb{S}$, one can consider algebraic operations over the sets by adding (Minkowski addition), multiplying, and convolving the support functions.

As observed before, the support functions of surfaces $\Sigma_{\boldsymbol{x}}$ corresponding to the Laplacian and Wachspress-Warren coordinates are given by $\rho(\boldsymbol{\nu})$ and $1/\rho(\boldsymbol{\nu})$, respectively, where $\rho(\boldsymbol{\nu})$ is the polar plot of $\partial\Omega$. Thus their product gives us the support function corresponding to the mean value coordinates and we can say that the Laplacian and Wachspress-Warren coordinates are dual w.r.t. to the multiplication of their corresponding support functions.

As noted in [MM06](Section 6, see also referneces to works of H. Görtler therein), the convolution of two support functions inherits properties of the factors. For the sake of simplicity, let us consider the 2D case. The convolution of $p(\theta)$ and $q(\theta)$ is given by

$$(p \otimes q)(\theta) = \frac{1}{2\pi} \int_0^{2\pi} p(\theta - \alpha) q(\alpha)\, d\alpha. \tag{52}$$

If $p(\theta)$ is centrally-symmetric, i.e., $p(\theta + \pi) \equiv p(\theta)$, so is convolution $p \otimes q$. If $q(\theta)$ is of constant-width (Fig. 2 gives an example of a constant-width curve generated from its support function),

$$q(\theta + \pi) + q(\theta) \equiv \text{const},$$

then $p \otimes q$ is also of constant width. Notice that a circle is the only centrally-symmetric set of constant width.

According to (46), if support function $p(\theta)$ of $\Sigma_{\boldsymbol{x}}$ is centrally-symmetric / constant-width, so is weighting function $w(x, \theta)$, and vice versa. Since the support functions corresponding to the weighted Gordon-Wixom coordinates are centrally-symmetric, then

"constant-width coordinates" are dual to the weighted Gordon-Wixom ones w.r.t. convolution (52).

7. Directions for further work

As shown in [SJW06], transfinite barycentric interpolation schemes can be viewed as limiting cases of their corresponding discrete versions, barycentric coordinates on polyhedral domains. Certainly the discrete case is more complex than the continuous one considered in this paper. For example, several different discrete counterparts of the transfinite barycentric coordinates are studied in [FHK06, JW05]. Establishing links between discrete barycentric coordinates and discrete Christoffel-Minkowski problems constitutes an interesting topic for further work.

In this paper, we haven't even touched on the transfinite Sibson coordinates [GF99] and Möobius-invariant interpolation [BE03]. Following [GW74], it would be also interesting to consider the Hermite data interpolation problem and study its relationships with fourth-order PDEs.

Another fascinating theme for future research consists of studying links between transfinite barycentric coordinates and continuous valuations on convex sets. [Had57, Sch93]. Some links between the Hadwiger characterization theorem of rigid motion invariant valuations [Had57] and barycentric coordinates are pointed out in [DMA02]. An interesting problem here is to study relations between barycentric coordinates and a more general class of translation invariant valuations [Sch96].

Acknowledgements

I am grateful to Kai Hormann, Tao Ju, and Joe Warren for fruitful discussions and for providing me with their manuscripts prior to publication. I would like to thank the anonymous reviewers for their comments and suggestions.

References

[ACGR02] Almansa A., Cao F., Gousseau Y., Rougé: Interpolation of digital elevation models using AMLE and related methods. *IEEE Transactions on Geoscience and Remote Sensing 40*, 2 (2002), 314–325. 6

[ACJ04] Aronsson G., Crandall M. G., Juutinen P.: A tour of the theory of absolutely minimizing functions. *Bull. Amer. Math. Soc. 41*, 4 (2004), 439–505. 6

[AO06] Arroyo M., Ortiz M.: Local maximum-entropy approximation schemes: a seamless bridge between finite elements and meshfree methods. *International Journal for Numerical Methods in Engineering 65*, 13 (2006), 2167–2202. 1

[BBM05] Berrut J.-P., Baltensperger R., Mittelmann H. D.: Recent developments in barycentric rational interpolation. In *Trends and Applications in Constructive Approximation*, D. H. Mache and J. Szabados and M. G. de Bruin, (Ed.), vol. 151 of *International Series of Numerical Mathematics*. Birkhäuser, Basel, 2005, pp. 27–52. 5

[BE03] Bern M. W., Eppstein D.: Möobius-invariant natural neighbor interpolation. In *Proc. 14th Symp. Discrete. Algorithms* (2003), pp. 128–129. 10

[BF34] Bonnesen T., Fenchel W.: *Theorie der Konvexen Körper*. Springer-Verlag, Berlin, 1934. 7, 9

[Bla30] Blaschke W.: *Vorlesung über Differentialgeometrie I*, dritte erweiterte auflage ed. Springer-Verlag, Berlin, 1930. 7

[Bus58] Busemann H.: *Convex Surfaces*. Interscience, New York, 1958. 7

[BVIK*97] Belikov V. V., V.D. Ivanov V. D., Kontorovich V. K., Korytnik S. A., Semenov A. Y.: The non-Sibsonian interpolation: a new method of interpolation of the values of a function on an arbitrary set of points. *Comput. Math. Math. Phys. 37*, 1 (1997), 9–15. 3

[CFL82] Christ N. H., Friedberg R., Lee T. D.: Weights of links and plaquettes in a random lattice. *Nucl. Phys. B 210*, 3 (1982), 337–346. 3

[CG67] Coxeter H. S. M., Greitzer S. L.: *Geometry Revisited*. Math. Assoc. Amer., Toronto - New York, 1967. 8

[Chr65] Christoffel E. B.: Uber die Bestimmung der Gestalt einer krummen. Oberfläche durch lokale messungen auf derselben. *J. Reine Angew. Math. 64* (1865), 193–209. 8

[CMS98] Caselles V., Morel J.-M., Sbert C.: An axiomatic approach to image interpolation. *IEEE Transactions on Image Processing 7*, 3 (1998), 376–386. 4, 6

[DM06] DeRose T., Meyer M.: *Harmonic coordinates*. Tech. Rep. Pixar Technical Memo #06-02, PIXAR, January 2006. 1

[DMA02] Desbrun M., Meyer M., Alliez P.: Intrinsic parameterizations of surface meshes. *Computer Graphics Forum 21*, 2 (2002), 209–218. Proc. Eurographics 2002. 3, 10

[Far02] Farin G.: A history of curves and surfaces in CAGD. In *Handbook of Computer Aided Geometric Design*, Farin G., Hoschek J., Kim M.-S., (Eds.). Elsevier, 2002, ch. 1. 1

[FH06] Floater M. S., Hormann K.: *Barycentric rational interpolation with no poles and high rates of approximation*. Tech. Rep. IfI-06-06, Department of Informatics, Clausthal University of Technology, May 2006. 5

[FHK06] Floater M. S., Hormann K., Kós G.: A general construction of barycentric coordinates over convex polygons. *Advances in Computational Mathematics* (2006). 4, 10

[Flo03] Floater M. S.: Mean value coordinates. *Computer Aided Geometric Design 20*, 1 (2003), 19–27. 1, 6

[FMR01] Farouki R. T., Moon H. P., Ravani B.: Minkowski geometric algebra of complex sets. *Geometriae Dedicata 85* (2001), 283–315. 8

[GF99] Gross L., Farin G. E.: A transfinite form of Sibson's interpolant. *Discrete Applied Mathematics 93*, 1 (1999), 33–50. 10

[GG02] Guan B., Guan P.: Convex hypersurfaces of prescribed curvature. *Annals of Mathematics 156* (2002), 655–674. 7

[GW74] Gordon W., Wixom J.: Pseudo-harmonic interpolation on convex domains. *SIAM J. Numer. Anal. 11*, 5 (1974), 909–933. 1, 4, 5, 10

[Had57] Hadwiger H.: *Vorlesungen über Inhalt, Oberfläche und Isoperimetrie*. Springer, Berlin, 1957. 10

[Her00] Herman R. A.: *A Treatise on Geometrical Optics*. Cambridge University Press, 1900. 8

[HF06] Hormann K., Floater M. S.: Mean value coordinates for arbitrary planar polygons. *ACM Transactions on Graphics* (2006). 1

[HS00] Hiyoshi H., Sugihara K.: An interpolant based on line segment Voronoi diagrams. In *JCDCG '98: Revised Papers from the Japanese Conference on Discrete and Computational Geometry* (2000), Springer-Verlag, pp. 119–128. 3

[JSW05a] Ju T., Schaefer S., Warren J.: A geometric construction of coordinates for convex polyhedra using polar duals. In *Third Eurographics Symposium on Geometry Processing* (Vienna, Austria, July 2005), pp. 181–186. 9

[JSW05b] Ju T., Schaefer S., Warren J.: Mean value coordinates for closed triangular meshes. *ACM Transactions on Graphics 24*, 3 (2005), 561–566. Proceedings of ACM SIGGRAPH 2005. 1, 2

[JW05] Ju T., Warren J.: *General Constructions of Barycentric Coordinates in a Convex Triangular Polyhedron*. Tech. rep., Washington University in St. Louis, November 2005. 10

[KFCO06] Klingner B. M., Feldman B. E., Chentanez N., O'Brien J. F.: Fluid animation with dynamic meshes. *ACM Transactions on Graphics 25*, 3 (2006). Proceedings of ACM SIGGRAPH 2006. 1

[MBLD02] Meyer M., Barr A., Lee H., Desbrun M.: Generalized barycentric coordinates on irregular polygons. *Journal of Graphics Tools 7*, 1 (2002), 13–22. 3

[Min03] Minkowski H.: Volumen und Oberfläsche. *Math. Ann. 57* (1903), 447–495. 7

[MM01] Martinez-Maure Y.: Hedgehogs and zonoids. *Advances in Mathematics 158*, 1 (2001), 1–17. 7

[MM06] Martinez-Maure Y.: Geometric study of Minkowski differences of plane convex bodies. *Canadian Journal of Mathematics* (2006). 9

[POMZ99] Peng D., Osher S., Merriman B., Zhao H.-K.: The geometry of wulff crystal shapes and its relations with Riemann problems. *Contemporary Mathematics 238* (1999), 251–303. 8

[PP99] Pinkall U., Polthier K.: Computing discrete minimal surfaces and their conjugates. *Experimental Mathematics 2*, 1 (1999), 15–36. 3

[Sch93] Schneider R.: *Convex Bodies: The Brunn-Minkowski Theory*. Cambridge Univ. Press, 1993. 7, 8, 9, 10

[Sch96] Schneider R.: Simple valuations on convex sets. *Mathematika 43* (1996), 32–39. 10

[She68] Shepard D.: A two-dimensional interpolation function for irregularly-spaced data. In *Proceedings of the 1968 23rd ACM national conference* (New York, NY, USA, 1968), ACM Press, pp. 517–524. 2, 4

[SJW06] Schaefer S., Ju T., Warren J.: A unified, integral construction for coordinates over closed curves. *Computer-Aided Geometric Design* (2006). A Special Issue on Discrete Geometry. Submitted. 1, 3, 9, 10

[SM06] Sukumar N., Malsch E. A.: Recent advances in the construction of polygonal interpolants. *Archives of Computational Methods in Engineering 13*, 1 (2006), 129–163. 1, 3

[STW04] Sheng W., Trudinger N., Wang X.-J.: Convex hypersurface of prescribed Weingarten curvatures. *Comm. in Analysis and Geometry 12*, 1 (2004), 213–232. 7

[Sug99] Sugihara K.: Surface interpolation based on new local coordinates. *Computer-Aided Design 31* (1999), 51–58. 3

[Suk03] Sukumar N.: Voronoi cell finite difference method for the diffusion operator on arbitrary unstructured grids. *International Journal for Numerical Methods in Engineering 57*, 1 (2003), 1–34. 4

[VF92] Vaillant R., Faugeras O. D.: Using extremal boundaries for 3-d object modeling. *IEEE Transactions on Pattern Analysis and Machine Intelligence 14*, 2 (1992), 157–173. 8

[Wac75] Wachspress E. L.: *A Rational Finite Element Basis*. Academic Press, New York, 1975. 3

[War96] Warren J.: Barycentric coordinates for convex polytopes. *Advances in Computational Mathematics 6*, 2 (1996), 97–108. 3

[War05] Wardetzky M.: Convergence of the cotan formula - an overview. Preprint, ZIB, 2005. To appear in 'Discrete Differential Geometry (A. I. Bobenko, J. M. Sullivan, P. Schröder, G. Ziegler, eds), Oberwolfach Seminars, Birkhäuser Basel. 4

[Wei84] Weingarten J.: *Über die Theorie der aufeinander abwickelbaren Oberflächen, Festschrift der technischen Hochschule*. Berlin, 1884. 7

[Wei94] Weickert J.: Anisotropic diffusion filters for image processing based quality control. In *Proc. Seventh European Conf. on Mathematics in Industry* (Stuttgart, 1994), Teubner, pp. 355–362. 6

[WSHD06] Warren J., Schaefer S., Hirani A. N., Desbrun M.: Barycentric coordinates for convex sets. *Advances in Computational and Applied Mathematics* (2006). To appear. 1, 3, 9